Second harmonic generation in microcrystallite films of ultrasmall Si nanoparticles

M. H. Nayfeh,[a] O. Akcakir, G. Belomoin, N. Barry, J. Therrien, and E. Gratton
Department of Physics, University of Illinois at Urbana-Champaign, 1110 West Green Street, Urbana, Illinois 61801

(Received 14 July 2000; accepted for publication 25 October 2000)

We dispersed crystalline Si into a colloid of ultrasmall nano particles (~1 nm), and reconstituted it into microcrystallites films on device-quality Si. The film is excited by near-infrared femtosecond two-photon process in the range 765–835 nm, with incident average power in the range 15–70 mW, focused to ~1 μm. We have observed strong radiation at half the wavelength of the incident beam. The results are analyzed in terms of second-harmonic generation, a process that is not allowed in silicon due to the centrosymmetry. Ionic vibration of or/and excitonic self-trapping on novel radiative Si–Si dimer phase, found only in ultrasmall nanoparticles, are suggested as a basic mechanism for inducing anharmonicity that breaks the centrosymmetry. © *2000 American Institute of Physics.* [S0003-6951(00)05452-8]

Recently, there has been interest in the nonlinear optical response and harmonic generation in silicon nanostructures,[1–3] stimulated by the discovery of the optical activity of porous silicon and the associated nanoscale structure of the material.[4] In measurements by Wang *et al.*[1] using 50 ps pulsed 1.06 μm excitation, it was suggested that a third harmonic photon (at 355 nm) is first generated in the core of nanostructures. The photoluminescence is then produced by a single photon excitation by the internally generated UV radiation. However, no radiation at the third harmonic was directly detectable in these experiments. In more recent measurements by Chin *et al.*[2] using short pulse at 0.870, 1.06, and 1.3 μm radiation, there was no evidence for second or third harmonic generation. The internal generation of second harmonic photon was ruled out since second harmonic generation is not allowed in bulk silicon due to the centrosymmetry. On the theoretical side, silicon is known to have negligible nonlinearity, being zero at the second order level (not allowed), and very small at the third order level.

In this letter, we report the observation of second harmonic generation in films of ultrasmall silicon nanoparticles, an effect that is not allowed in bulk silicon due to the centrosymmetry. Silicon was dispersed into a suspension nanoparticle colloid of ~1 nm across.[5,6] The particles were then reconstituted to create large, thick, uniform, and under control layers of microcrystallites on device quality Si substrates. The film is excited by near-infrared femtosecond two photon process at 750–830 nm. Ionic vibration of or/and excitonic self-trapping on radiative Si–Si dimer phase,[7,8] found only in ultrasmall nanoparticles, are suggested as a basic mechanism for inducing anharmonicity that breaks the centrosymmetry which forbids the process in bulk.

The substrates were (100) oriented, 1–10 Ω cm resistivity, *p*-type boron doped silicon, laterally anodized in hydrogen peroxide and HF acid[5,6,9] while advancing the wafer in the etchant at a reduced speed of ~1 mm per hour. Subsequent immersion in an ultrasound acetone or water bath crumbles the top film into ultrasmall particles. When it is excited by a nanosecond radiation at 355 nm, deep blue emission is observed with the naked eye, in room light. Direct imaging, using high resolution transmission electron microscopy, of a thin graphite grid which was coated with the particles shows that the particles are 1 nm in diameter with 10% dispersion.[10] Electron photospectroscopy and infrared Fourier spectroscopy show that the particles are composed of silicon, dominated by hydrogen termination with less than 10% oxygen. The particles are precipitated from a water solvent to reconstitute the material into a thin film (a few microns thick) on a device quality silicon or glass. Under solidification the film shatters. Optical imaging (see Fig. 1) shows that colloidal crystals of 50–100 μm across. We used mode locked femtosecond Ti:sapphire near-infrared laser of 150 fs pulse duration at a repetition rate of 80 MHz. At the

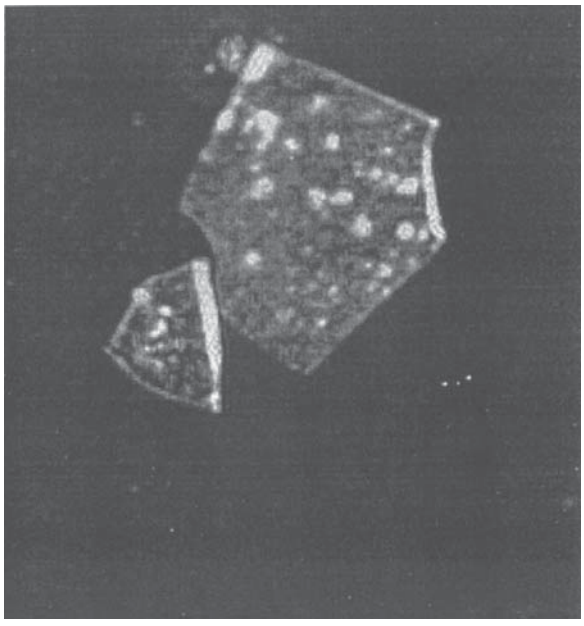

FIG. 1. 275 μm×300 μm optical image, showing two microcrystallite fragments from a film reconstituted from the silicon nanoparticles.

[a]Electronic mail: m-nayfeh@uiuc.edu

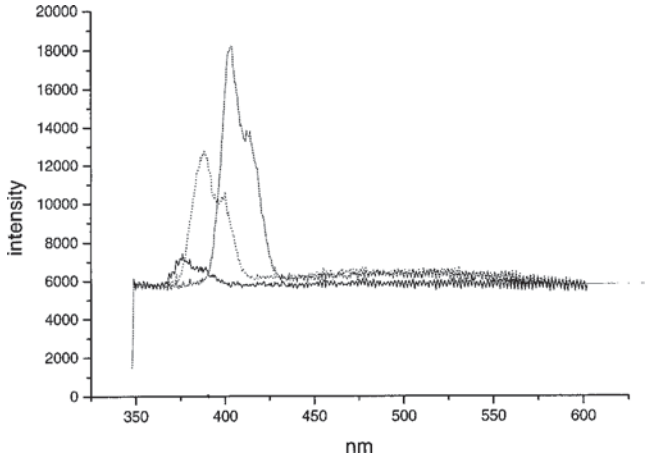

FIG. 2. Emission spectra for the three excitation wavelengths 780 (solid), 800 (dot), and 832 (dense dot) nm (at different incident intensities). Each shows a peak with a shoulder on the red wing. The shoulders are set at 390, 400, and 416 nm, respectively.

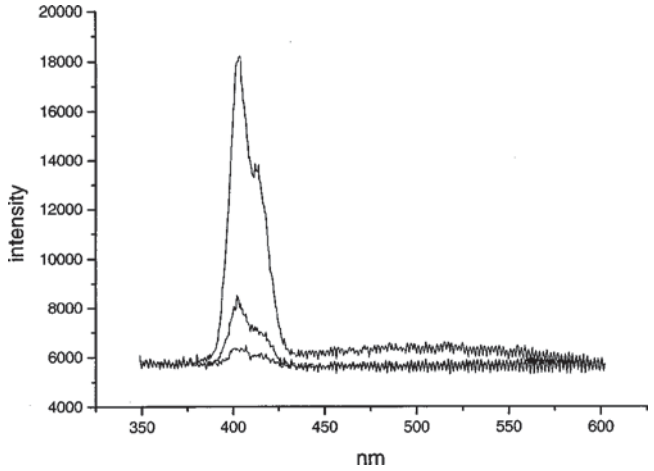

FIG. 3. Emission spectra of increasing strength recorded at 832 nm for 15, 29, and 59 mW incident power, showing a quadratic dependence.

target, the average power, 5–300 mW, is focused to diffraction limited spots ~1 μm diameter, giving an average intensity of 2×10^5 to $4\sim10^7$ W/cm^2 (peak intensity of $2\times10^{10}-4\sim10^{12}$ W/cm^2). The configuration of the excitation and detection optics is such that the incident beam strikes the sample in near normal incidence, and the emission is detected in the backscattering direction (180° relative to the incident beam). The silicon substrate provides a reflectivity of ~0.5 at 400 nm, and 0.4 at 780 nm. Thus the signal is partly due to direct backscattering and partly due to reflected forward scattering. The beam–sample interaction is viewed via an optical microscope (×10) and the excitation light was raster scanned. Emission is detected by a photomultiplier and stored in a two-dimensional array. The spectral response is analyzed with a resolution of 4 Å by a grating dispersive element and a charge sensitive detector cooled to 0° to reduce the dark current count.

Figure 2 gives the emission spectra for the three excitation wavelengths 780, 800, and 832 nm (of different incident intensities). Each shows a double peak spectrum. The ratio of the peak is ~0.60, essentially flat with incident intensity. Those and other measurements show that the emitted wavelength tracks the incident wavelength. The peaks at 390, 400, and 416 nm, respectively, are at half the wavelengths of the incident beam (second harmonic). The peaks at 380, 390, and 406 nm are blueshifted by 10 nm from the second harmonic peak. We find no measurable harmonic generation from control Si substrates with no nanoparticles deposited, and that the incident beam does not have a double peak profile. We examined the power dependence of the emission. The spectra (of increasing strength) shown in Fig. 3 were recorded using radiation at 832 nm wavelength at, respectively, 15, 29, and 59 mW incident intensity, shows a quadratic response with incident intensity. However, in some measurements, the response was found slightly subquadratic which we may attribute to sample degradation or damage.

A plausible mechanism for the second harmonic generation may be derived from a recent model.[7,8] Allan *et al.*[7] theoretically discovered, using first principle calculations, the formation, in ultrasmall nanocrystallites (<1.75 nm), of new stable configuration (or phase), distinct from but interconnected to diamond-like structure by a potential barrier. It is based on pairing of surface atoms to form intrinsic Si–Si dimer bonds that act as self-trapped excitons on a single bond. Figure 4 gives a schematic of the interatomic potential of the bond[7] and the various pathways for absorption and emission in a 1.03 nm diameter particle.[8] To estimate the anharmonicity, we expand the interatomic potential as a function of the bond length (Fig. 4) about its minimum. $V(r)=ar^2+Dr^3$ where r is the displacement from the potential minimum, and the second term is the first anharmonic term. The fit gives $mD\sim5.1\times10^{13}$ V/m^3, where m is the mass of the electron. For centrosymmetric material, the coefficient D vanishes. From D we can determine the frequency independent nonlinear optical coefficient $\delta=mD/2e^3N^2$

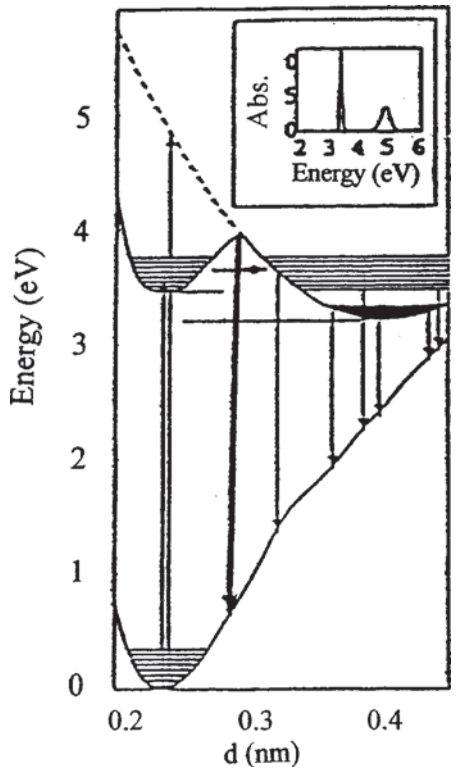

FIG. 4. Schematic of the interatomic potential of the Si–Si bond and the various pathways for absorption and emission in a 1.03 nm diameter particle.

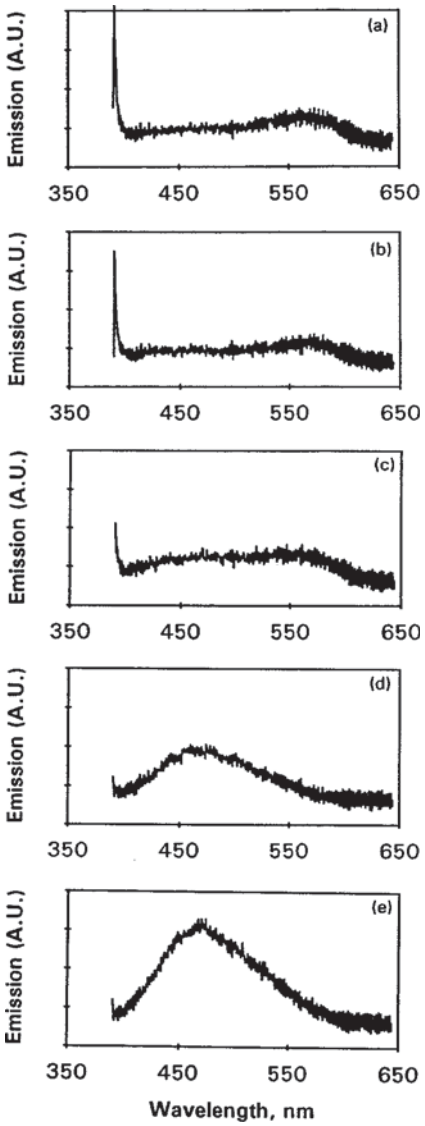

FIG. 5. Emission spectra at the same intensity and wavelength from several spots or/and microcrystallite fragments. The harmonic peak anticorrelates with a blue band at 400–500 nm but correlates with the green/yellow band at 510–625 nm. No obvious differences in the optical images of the fragments that may explain the differences in the spectral distributions.

where N is the density of electrons that contribute to the polarization.[11] This gives $\delta \sim 7\times 10^{13}$ MKS for $N=6\times 10^{28}/\mathrm{m}^3$. This is a large coefficient in view of the fact that the mean value of the parameter δ for 25 noncentrosymmetric crystals known for second harmonic generation is 2×10^9, insuring a large polarization even for smaller susceptibilities. The polarization at the second harmonic is proportional to δ and to the susceptibilities at the frequencies ω and 2ω: $P^{(2\omega)}=1/2d^{(2\omega)}E_0^2\cos 2\omega$, where $d^{(2\omega)}=\delta(\chi^{(\omega)})^2\chi^{(2\omega)}$, and $\chi^{(\omega)}$ is the linear susceptibility.

To explore the origin of the blueshifted peak, we check the characteristic vibration frequency of the system. We previously calculated the vibration structure of the dimers,[8] yielding 42 meV for the vibrational spacing. For incident wavelength of ~780 nm, this vibration energy produces an anti-Stokes line at 759.4 nm, with a shift of 20.6 nm. Harmonic generation of the Raman shifted radiation gives a line at 380 nm, with a shift of 10.3 nm. Thus it is possible that the blueshifted peak is a higher order nonlinear coherent process such as stimulated anti-Stokes scattering.[11,12] Although Stokes lines are expected to be more efficient than anti-Stokes lines, there are no resolved Stokes peaks.

In cataloging the response from different parts of the shattered film, we noticed some relationship between the second harmonic and the luminescence. However, we noted no noticeable differences in the optical image of the film that might be correlated with the spectral width or distribution of the emission spectrum. The spectra in Figs. 2 and 3 show strong harmonic generation. Spectra in general, have a harmonic peak, a blue band 400–500 nm, and a weaker green/yellow band 510–623 nm. Figure 5 shows several spectral from different parts of the film; they show the harmonic peak anticorrelates with the blue band but correlates with the green/yellow band. Is the disappearance of the harmonic generation due to internal reabsorption to produce the luminescence, or is it inhibited dynamically in favor of the luminescence channels? or due to phase matching conditions? Those require information on the fundamental structure of the nanoparticles as well as the electromagnetic part of the problem, including issues of phase matching, in addition to the feedback by the silicon substrate.

In conclusion, we dispersed Si into a colloid of ultrasmall nanoparticles (~1 nm), and reconstituted into microcrystallites on device-quality Si. The film is excited by near-infrared femtosecond two-photon process at 750–830 nm with the radiation focused to ~1 μm. We have observed narrow radiation at half the incident wavelength. The results are discussed in terms of second-harmonic generation. Ionic vibration of or/and excitonic trapping on radiative Si–Si dimer phase, found only in ultrasmall nanoparticles, are suggested as a basic mechanism for inducing anharmonicity that breaks the centrosymmetry.

The authors acknowledge State of Illinois Grant IDCCA No. 00-49106, the U. S. Department of Energy Grant No. DEFG02-91-ER45439, and the National Institute of Health (RR03155) and the University of Illinois at Urbana-Champaign.

[1] J. Wang, H.-B. Jiang, W.-C. Wang, J.-B. Zheng, F.-L. Zhang, P.-H. Hao, X.-Y. Hou, and X. Wang, Phys. Rev. Lett. **69**, 3252 (1992).
[2] R. P. Chin, Y. R. Shen, and V. Petrova-Koch, Science **270**, 776 (1995).
[3] M. Nayfeh, O. Akcakir, J. Therrien, Z. Yamani, N. Barry, W. Yu, and E. Gratton, Appl. Phys. Lett. **75**, 4112 (1999).
[4] L. T. Canham, Appl. Phys. Lett. **57**, 1046 (1990).
[5] O. Akcakir, J. Therrien, G. Belomoin, N. Barry, E. Gratton, and M. Nayfeh, Appl. Phys. Lett. **76**, 1857 (2000).
[6] G. Belomoin, J. Therrien, and M. H. Nayfeh, Appl. Phys. Lett. **77**, 779 (2000).
[7] G. Allan, C. Delerue, and M. Lannoo, Phys. Rev. Lett. **76**, 2961 (1996).
[8] M. Nayfeh, N. Rigakis, and Z. Yamani, Phys. Rev. B **56**, 2079 (1997); Mater. Res. Soc. Symp. Proc. **486**, 243 (1998).
[9] Z. Yamani, H. Thompson, L. AbuHassan, and M. H. Nayfeh, Appl. Phys. Lett. **70**, 3404 (1997); D. Andsager, J. Hilliard, J. M. Hetrick, L. H. AbuHassan, M. Plisch, and M. H. Nayfeh, J. Appl. Phys. **74**, 4783 (1993); Z. Yamani, S. Ashhab, A. Nayfeh, and M. N. Nayfeh, *ibid*. **83**, 3929 (1998).
[10] Z. Yamani, A. Alaql, J. Therrien, O. Nayfeh, and M. H. Nayfeh, Appl. Phys. Lett. **74**, 3483 (1999).
[11] A. Yariv, *Quantum Electronics* (Wiley, New York, 1975).
[12] Y. R. Shen and N. Bloembergen, Phys. Rev. **137**, A1787 (1965); J. A. Armstrong, N. Bloembergen, J. Dunning, and P. S. Pershan, *ibid*. **127**, 1918 (1962).